On the Gain of Joint Decoding for Multi-Connectivity

Albrecht Wolf, Philipp Schulz, David Öhmann, Meik Dörpinghaus, and Gerhard Fettweis
Vodafone Chair Mobile Communications Systems, Technische Universität Dresden, Germany
E-mails: {albrecht.wolf, philipp.schulz2, david.oehmann, meik.doerpinghaus, gerhard.fettweis}@tu-dresden.de

***Abstract*—Multi-connectivity is considered to be key for enabling reliable transmissions in future wireless networks. Transmission reliability depends on the used combining algorithm such as joint decoding (JD), maximum selection combining (MSC), and maximum ratio combining (MRC). To compare the performance of these combining algorithms we derive their outage probabilities based on distributed source coding. The outage probability is analytically described depending on the number of links, the modulation scheme, the code rate, and the received signal-to-noise-ratios (SNR). We show that JD requires less transmit power than MRC and MSC to achieve a given target outage probability.**

I. Introduction

Fifth-generation mobile networks (5G) will face several challenges to cope with emerging application scenarios [1] in the context of ultra-reliable low latency communications (URLLC). These requirements pose a massive challenge on the physical layer. In fourth-generation mobile networks (4G), reliability is obtained by the hybrid automatic repeat request procedure, which retransmits erroneously received packets. However, the tight timing constraint of URLLC does not endorse multiple retransmissions.

Multi-connectivity (MC) is seen as a promising concept to enable URLLC in 5G [2] by establishing multiple diversity branches in the frequency domain. Different combining algorithms are known to take advantage of the multiple diversity branches. In this work, we concentrate on three combining algorithms, which are joint decoding (JD), maximum selection combining (MSC), and maximum ratio combining (MRC), and derive their outage probabilities. We establish a remarkably simple, yet accurate analytical framework depending on the number of links, the spectral efficiency (associated with the code rate and the modulation scheme), and the received signal-to-noise ratio (SNR). By deriving the SNR gain, we show that JD outperforms MSC and MRC. Next, we briefly describe MC and JD, and then outline our approach and our contributions.

Multi-Connectivity: In wireless communications, MC concepts have been mainly developed and applied for increasing data rates and capacity. Various ways exist to realize MC and we distinguish between two types, namely, intra- and inter-frequency MC. Established principles realizing intra-frequency MC are single frequency networks [3] and coordinated multi-point [4]. On the other hand, for inter-frequency MC, where one or more base stations (BSs) use multiple carrier frequencies to simultaneously transmit signals to a single user, concepts such as carrier aggregation and dual connectivity have been introduced to make use of multiple so-called component carriers. As indicated before, existing realizations of MC are mainly used for enhancing data rates and capacities, i.e., different information is transmitted over each link (multiplexing). However, multiple connections can also be utilized to enhance the reliability, i.e., the same information is transmitted over all links in parallel (diversity).

Recently, research on URLLC is emerging considerably; nevertheless, there are only a few works focusing on a detailed analysis of MC and its impact on reliability. In [5], it is concluded that packet duplication across multiple connections is a suitable technique to achieve high reliability. Pocovi et al. evaluate intra-frequency MC in system simulations to illustrate how the SINR and the reliability is improved [6].

Motivated by the potential of MC to satisfy the URLLC requirements, we investigate a system model that complies with MC architectures. The multiple diversity branches that correspond to an orthogonal multiple access channel (MAC) are realized by different carrier frequencies. Thus, the information can, in the best case, be delivered in a single time slot, which helps satisfying the URLLC requirements.

Joint Decoding: The performance improvement of JD can be reasoned by distributed source coding (DSC). Slepian and Wolf [7] were the first to characterize the problem of distributed encoding of multiple correlated sources. In their seminal paper, the rate region for the lossless distributed encoding of two correlated sources was derived.

Motivated by the capabilities of practical JD schemes (see, e.g., [8]) Matsumoto et al. established an analytical framework to evaluate their performance. In [9] the JD outage performance was analyzed for a three-node decode-and-forward relaying system allowing intra-link errors (DF-IE). The analysis was based on DSC and the source-channel separation theorem [10, Th. 3.7]. In [11] and [12] the analysis was extended to a DF-IE system model with an arbitrary number of relays, with and without a direct link between source and destination, respectively.

Problem Statement: A convenient way to analyze the JD performance improvement is to evaluate the required transmit

This work was supported in part by the Federal Ministry of Education and Research within the programme "Twenty20 - Partnership for Innovation" under contract 03ZZ0505B - "fast wireless" and in part by the German Research Foundation (DFG) within the SFB 912 "Highly Adaptive Energy-Efficient Computing (HAEC)".

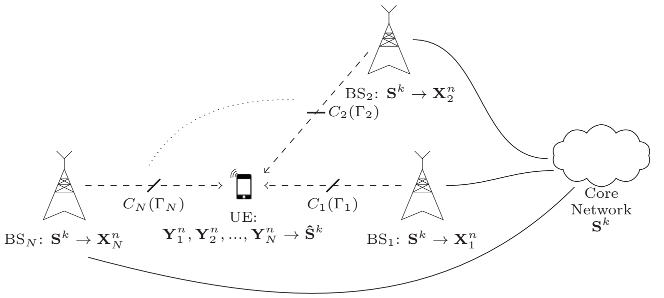

Fig. 1: System model with a single UE, N base stations, and a core network for downlink.

power of JD, MSC, and MRC achieving a given target outage probability. Eventually, we are interested in the transmit power offset between JD and MSC/MRC, which we refer to as SNR gain. This paper aims to develop a better understanding of this SNR gain in block-fading orthogonal MACs in the context of MC.

Contributions of this Work: We consider the MC architecture as a DSC setup, consisting of one source which is independently compressed at different terminals and the decoder aims to perfectly reproduce the source. This allows us to use Slepian-Wolf's admissible rate region [7] which we adjust to the MC architecture. Based on the approach in [9] we then derive the outage probability for JD, MSC and MRC. The outage probability is a quantitative parameter for transmission reliability. Eventually, we establish a remarkably simple, yet accurate analytical description of the outage probability depending on the number of links, the modulation scheme, the code rate, and the received SNR. We show the SNR gain of JD in comparison to MSC and MRC while achieving the same outage probability.

Notation and Terminology: In what follows, Pr$[\cdot]$ denotes probability, $f_X(x)$/$p_X(x)$ is the probability density function (pdf)/probability mass function (pmf) of a continuous/discrete random variable (RV) X. For the sake of simplicity, we denote the pdf/pmf as $f(x)$/$p(x)$ when this does not create any confusion. x is a sample realization of a RV X and its cardinality is denoted by $|\mathcal{X}|$. Vectors containing a temporal sequence of X and x are denoted in bold letters, $\mathbf{X}^n$ and $\mathbf{x}^n$, respectively, where the superscript n denotes the vector length. In general, a set $\mathbf{A}$ contains elements $a_{(\cdot)}$, as in $\mathbf{A} = \{a_1, a_2, ..., a_{|\mathbf{A}|}\}$. To simplify notations, we define an indexed series: (i) of RVs as $A_{\mathcal{S}} = \{A_i | i \in \mathcal{S}\}$, and (ii) of random vectors as $\mathbf{A}_{\mathcal{S}} = \{\mathbf{A}_i | i \in \mathcal{S}\}$. We denote i as a source index, t as a time index, and $\mathcal{L}_x[f(x)](p)$ as the Laplace transform of $f(x)$.

II. System Model

A. Multi-Connectivity System Model

We consider a MC cellular network, as shown in Fig. 1, consisting of a core network, N base stations (BS$_i, \forall i \in \mathcal{N} = \{1, 2, ..., N\}$), communicating to a single user equipment (UE). The core network coordinates the data transmissions from and to the UE. Connections between the core network and each BS are realized by backhaul links, and connections between each BS and UE by wireless links. The achievable transmission rate over the ith wireless link depends on its capacity $C_i(\Gamma_i)$ and, thus, on its received SNR Γ_i. In the system model, we distinguish between down- and uplink as follows:

a) Downlink: The downlink system model, as illustrated in Fig. 1, has one binary memoryless source, denoted as $[S(k)]_{t=1}^{\infty}$, with the k-sample sequence being represented in vector form as $\mathbf{S}^k = [S(1), S(2), ..., S(k)]$. When appropriate, for simplicity, we shall drop the temporal index of the sequence, denoting the source merely as S. By assumption S takes values in a binary set $\mathcal{B} = \{0, 1\}$ with uniform probabilities, i.e., Pr$[S = 0]$ = Pr$[S = 1] = 0.5$, $\forall i \in \mathcal{N}$. Therefore the entropy of the sequence is

$$^1/_k H(\mathbf{S}^k) = H(S) = 1. \tag{1}$$

The source sequence $\mathbf{S}^k$ originating from the core network is encoded at N BSs. The ith transmit sequence at BS i, denoted as $\mathbf{X}_i^n$, is sent to the UE over an orthogonal MAC. The decoder at the UE retrieves the source sequence $\mathbf{S}^k$ from the received sequences $\mathbf{Y}_i^n, \forall i \in \mathcal{N}$.

b) Uplink: The uplink system model is similar to the downlink, except that the source sequence is originated from the UE, and the received sequences $\mathbf{Y}_i^n, \forall i \in \mathcal{N}$, are decoded at the core network to retrieve the source sequence $\mathbf{S}^k$. Similar to the downlink, the ith transmit sequence $\mathbf{X}_i^n$ is sent from the UE to the ith BS over an orthogonal MAC.

B. Link Model

Instead of sending multiple sequences at different time instances, i.e., coding in time, we use multiple frequency channels to transmit the information. Thus, the information can, in the best case, be delivered in a single time slot, which helps satisfying the URLLC requirements. The frequency channels can be realized by using different channels within a single frequency band or, alternatively, by using channels of different frequency bands, cf. inter-frequency MC in Section I. According to [13], the small-scale fading of two signals is approximately uncorrelated if their frequencies are at least separated by the coherence bandwidth, which is confirmed, for instance, by measurement results in [14]. In the following, we assume that the used frequency resources are at least separated by the coherence bandwidth. Thus, the channels are orthogonal and fade independently. Furthermore, to cope with the low latency constraint in URLLC, we consider relatively short encoded sequences. As a result, the length of an encoded sequence is less than or equal to the length of a fading block of the block Rayleigh fading. Moreover, the signals are transmitted from or to different BSs, which leads to individual average SNR values.

As argued, we can assume that the sequences $\mathbf{X}_i^n$, $\forall i \in \mathcal{N}$, are transmitted (up- and downlink) over independent channels undergoing block Rayleigh fading and additive white Gaussian noise (AWGN) with mean power N_0. The pdf of the received SNR Γ_i is given by

$$f_{\Gamma_i}(\gamma_i) = \frac{1}{\bar{\Gamma}_i} \cdot \exp\left(-\frac{\gamma_i}{\bar{\Gamma}_i}\right), \quad \text{for } \gamma_i \geq 0, \tag{2}$$

with the average SNR $\bar{\Gamma}_i$ being obtained as

$$\bar{\Gamma}_i = \frac{P_i}{N_0} \cdot d_i^{-\eta}, \tag{3}$$

where P_i is the transmit power per channel, d_i is the distance between BS_i and the UE, and η is the path loss exponent. The channel state information is assumed to be known at the receiver.

The total transmit power P_T is equally allocated to all channels such that $P_i = {}^1/_N P_\text{T}, \forall i \in \mathcal{N}$. Then, from (3) the average received SNR at the receiver can be written as

$$\bar{\Gamma}_i = \frac{{}^1/_N P_\text{T}}{N_0} \cdot d_i^{-\eta}. \tag{4}$$

In addition, we define the average system transmit SNR as ${}^{P_\text{T}}/_{N_0}$, i.e, normalizing all distances d_i to one. We shall use the total transmit power constraint for comparison of different configurations later on.

III. Preliminaries

In this section, we outline how we connect DSC to the outage analysis of the MC system model. First, we recall the Slepian-Wolf admissible rate region, which will then be applied to the MC system model; and second, we illustrate the rate to SNR mapping.

A. Slepian-Wolf Theorem

Slepian and Wolf [7] considered a source coding problem where the decoder aims at perfectly reproducing two correlated sources, which are independently compressed at two terminals. In their seminal paper, the admissible rate region for this problem was derived. A simple proof of the Slepian-Wolf result with extension to an arbitrary number of correlated sources was presented by Cover in [15].

Theorem 1 (Generalized Slepian-Wolf theorem [15]) *In order to achieve lossless compression of N correlated sources $S_1, S_2, ..., S_N$, the source code rates $R_i, \forall i \in \mathcal{N}$, measured in bits per source sample, should satisfy the following conditions*

$$\textstyle\sum_{i\in\mathcal{S}} R_i \geq H\left(\{S_i | i \in \mathcal{S}\} | \{S_j | j \in \mathcal{S}^c\}\right), \forall \mathcal{S} \subseteq \mathcal{N}, \tag{5}$$

where $\mathcal{S}^c$ denotes the complement of $\mathcal{S}$.

If all sources are identical the Slepian-Wolf setup corresponds to the MC system model, i.e., the Slepian-Wolf rate region in (5) simplifies to

$$\textstyle\sum_{i=1}^{N} R_i \geq H(S) = 1 \tag{6}$$

The set of N-tuples $R_1, ..., R_N$ that satisfy all the constraints in (6) is referred to as the MC admissible rate region $\mathcal{R}_\text{MC}$.

For comparison, lossless compression of source S, considering a single link, can be achieved if the source code rate R_i satisfies the following condition, see, e.g., [10, Theorem 3.4]

$$R_i \geq H(S) = 1. \tag{7}$$

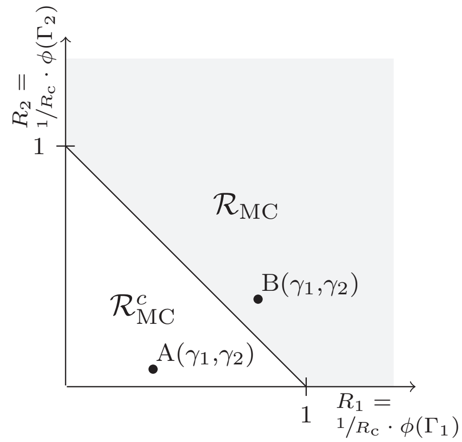

Fig. 2: MC admissible rate region and SNR to rate mapping.

B. Mapping: SNR to Rate

For a point-to-point communication system where a transmitter wishes to communicate k symbols of an uncompressed source S over a discrete memoryless channel in n transmissions so that the receivers can reconstructed the source symbols within a distortion constraint D, it is proven that performing source and channel coding separately is asymptotically optimal, i.e., for $k \to \infty$ [10, Theorem 3.7]. Therefore, the maximum achievable value of the transmission rate R_i is then related to the received SNR Γ_i, based on the block Rayleigh fading assumption, by

$$R_i = \frac{1}{{}^k/_n} C_i(\Gamma_i) = \frac{1}{R_{i,\text{c}}} \phi(\Gamma_i) \tag{8}$$

where the capacity $C_i(\Gamma_i)$ for an AWGN channel is given by $\phi(\Gamma_i) = \log_2(1 + \Gamma_i)$. $R_{i,\text{c}}$ represents the spectral efficiency, measured in source samples per channel input symbol, associated with the modulation scheme $R_{i,\text{M}} = \log_2(M)$, with the cardinality of the channel input symbol alphabet M, and the channel code rate $R_{i,\text{cod}}$, i.e., $R_{i,\text{c}} = R_{i,\text{M}} \cdot R_{i,\text{cod}}$. If not otherwise stated, for simplicity, we shall assume $R_{i,\text{c}} = R_\text{c}$.

Fig. 2 illustrates the SNR to rate mapping for $N = 2$. Lets assume that we have two received SNR realizations, i.e., 2-tuple (γ_1, γ_2). With (8) we can map the received SNR realizations into the transmission rate domain, i.e., 2-tuple $({}^1/_{R_\text{c}} \cdot \phi(\gamma_1), {}^1/_{R_\text{c}} \cdot \phi(\gamma_2))$. In Fig. 2 we illustrated two different 2-tuples at point A and point B. In addition, Fig. 2 illustrates the MC admissible rate region $\mathcal{R}_\text{MC}$ and its counterpart the MC inadmissible rate region $\mathcal{R}_\text{MC}^c$. Both regions are separated from each other by the rate constraint in (6), i.e., $R_1 + R_2 = 1$.

IV. Outage Probability

In this section, we consider three combining algorithms, which are JD, MSC and MRC. A combining algorithm can exploit the correlation of the received sequences to improve the transmission reliability, i.e., achieve a lower outage probability. Based on the Slepian-Wolf theorem and the SNR to rate mapping we establish an outage analysis for all three schemes in the context of MC.

A. Joint Decoding

We aim to derive an exact expression for the JD outage probability based on the MC admissible rate region, which we achieve in integral form. Unfortunately, the integral form cannot be solved in closed form, thus we give an approximation for the high SNR regime.

An outage event occurs whenever the transmission rate N-tuple $R_1, ..., R_N$ falls outside the MC admissible rate region $\mathcal{R}_{\text{MC}}$. Using (8), the sum rate constraint in (6) that defines $\mathcal{R}_{\text{MC}}$ can be mapped into a set of equivalent SNR constraints. Fig. 2 illustrates this approach for $N = 2$. The received SNR realizations, i.e., the 2-tuple (γ_1, γ_2), at point A, are transformed into transmission rates, i.e., the 2-tuple $(1/R_c \cdot \phi(\gamma_1), 1/R_c \cdot \phi(\gamma_2))$. Since the transmission rate 2-tuple at point A is outside the MC admissible rate region $\mathcal{R}_{\text{MC}}$ an outage event occurs, i.e., the joint decoder cannot perfectly reproduce the source sequence $\mathbf{S}^k$. The transmission rate 2-tuple at point B is inside the MC admissible rate region $\mathcal{R}_{\text{MC}}$, i.e., the joint decoder can perfectly reproduce the source sequence $\mathbf{S}^k$.

For an arbitrary number of BSs, the joint decoding outage probability can be calculated as follows:

$$P^{\text{out}}_{\text{JD},N} = \Pr\left[0 \le R_1 + R_2 + ... + R_N < 1\right] \quad (9)$$
$$= \Pr\left[0 \le \phi(\Gamma_1) < R_c, 0 \le \phi(\Gamma_2) < R_c - \phi(\Gamma_1), ..., 0 \le \phi(\Gamma_N) < R_c - \phi(\Gamma_1) - ... - \phi(\Gamma_{N-1})\right] \quad (10)$$
$$= \int_{\gamma_1=0}^{2^{R_c}-1} \int_{\gamma_2=0}^{2^{R_c-\phi(\gamma_1)}-1} ... \int_{\gamma_N=0}^{2^{R_c-\phi(\gamma_1)-...-\phi(\gamma_{N-1})}-1} f(\gamma_1) f(\gamma_2) ... f(\gamma_N) \mathrm{d}\gamma_N ... \mathrm{d}\gamma_2 \mathrm{d}\gamma_1. \quad (11)$$

The steps are justified as follows: (9) is the constraint on the sum rate in (6); in (10) the rate constraint is mapped into the SNR constraint with use of (8) and the sum constraint is separated into individual constraints; in (11) the bounds are transformed with $\phi^{-1}(y) = 2^y - 1$ and the probability of outage is established in integral form with the assumption that the received SNRs are independent and the pdf $f(\gamma_i)$ in (2). Although the outage expression in (11) cannot be solved in closed form, an asymptotic solution can be derived at high SNR

$$P^{\text{out}}_{\text{JD},N} \approx \frac{A_N}{\bar{\Gamma}_1 \bar{\Gamma}_2 ... \bar{\Gamma}_N}, \quad \text{where} \quad (12)$$
$$A_N = (-1)^N \left(1 - 2^{R_c} \cdot e_N\left(-R_c \ln(2)\right)\right). \quad (13)$$

Here, $e_N(x) = \sum_{n=0}^{N-1} \frac{x^n}{n!}$ is the exponential sum function. For more details, we refer to the derivations in [16, Appendix A].

B. Maximum Selection Combining

For MSC [17] at each time instant only the channel with the maximum transmission rate $R_{\max} = \max(R_1, R_2, ..., R_N)$ is selected. If $R_{\max}$ does not satisfy the rate constraint in (7) an outage occurs. In other word, each received source sequence is decoded individually and no received source sequence can be perfectly reproduced. The outage probability can be calculated as follows:

$$P^{\text{out}}_{\text{MSC},N} = \Pr\left[0 \le R_{\max} < 1\right] \quad (14)$$
$$= \Pr\left[0 \le \phi(\Gamma_{\max}) < R_c\right] \quad (15)$$
$$= \Pr[0 \le \phi(\Gamma_1) < R_c, 0 \le \phi(\Gamma_2) < R_c, ..., 0 \le \phi(\Gamma_N) < R_c] \quad (16)$$
$$= \prod_{i=1}^{N} \int_{\gamma_i=0}^{2^{R_c}-1} f(\gamma_i) \mathrm{d}\gamma_i \quad (17)$$
$$= \prod_{i=1}^{N} \left(1 - \exp\left(-A_1/\bar{\Gamma}_i\right)\right), \quad (18)$$

where $A_1 = 2^{R_c} - 1$. The steps are justified as follows: (14) is the constraint on the rate in (7); (15) - (17) follow similar arguments as in (10) and (11) and the multiple integral can be rewritten as the product of single integrals, since the integral domain is normal and RVs $\Gamma_i, i \in \mathcal{N}$ in (16) are independent; (18) is the closed-form solution of the integral in (17).

C. Maximum Ratio Combining

For MRC [17] all received symbols are coherently added. The sum of all symbols is then decoded. We can apply the point-to-point communication system assumption in the source-channel separation theorem [10, Theorem 3.7] if we define an auxiliary RV, namely the total received SNR Γ_{MRC} as

$$\Gamma_{\text{MRC}} = \sum_{i=1}^{N} \Gamma_i. \quad (19)$$

The pdf of the received SNR Γ_{MRC} is given by

$$f_{\Gamma_{\text{MRC}}}(\gamma_{\text{MRC}}) = f_{\Gamma_1}(\gamma_1) * f_{\Gamma_2}(\gamma_2) * ... * f_{\Gamma_N}(\gamma_N) \quad (20)$$
$$= \mathcal{L}_p^{-1}\left[\mathcal{L}_{\gamma_1}\left[f_{\Gamma_1}(\gamma_1)\right](p) \cdot \mathcal{L}_{\gamma_2}\left[f_{\Gamma_2}(\gamma_2)\right](p) \cdot ... \cdot \mathcal{L}_{\gamma_N}\left[f_{\Gamma_N}(\gamma_N)\right](p)\right](\gamma_{\text{MRC}}) \quad (21)$$
$$= \frac{\gamma_{\text{MRC}}^{(N-1)}}{(N-1)! \cdot \bar{\Gamma}^N} \exp\left(-\frac{\gamma_{\text{MRC}}}{\bar{\Gamma}}\right) \quad (22)$$

The steps are justified as follows: for (20) the pdf of a sum of RVs is the convolution of their pdfs; for (21) a convolution of functions is a multiplication of their Laplace transforms where $\mathcal{L}_{\gamma_i}\left[f_{\Gamma_i}(\gamma_i)\right](p) = 1/(\bar{\Gamma}_i p + 1)$. The result in (22) holds for $\bar{\Gamma}_1 = ... = \bar{\Gamma}_N = \bar{\Gamma}$ which we assume here for simplicity. With the total received SNR Γ_{MRC} we can assume a point-to-point communication system and thus the outage probability can be calculated as follows:

$$P^{\text{out}}_{\text{MRC},N} = \Pr\left[0 \le R_{\text{MRC}} < 1\right] \quad (23)$$
$$= \Pr\left[0 \le \phi(\Gamma_{\text{MRC}}) < R_c\right] \quad (24)$$
$$= \int_{\gamma_{\text{MRC}}=0}^{2^{R_c}-1} f(\gamma_{\text{MRC}}) \mathrm{d}\gamma_{\text{MRC}} \quad (25)$$
$$P^{\text{out}}_{\text{MRC},N} = 1 - \exp\left(-\frac{A_1}{\bar{\Gamma}}\right) \left(\sum_{i=1}^{N} \frac{\left(A_1/\bar{\Gamma}\right)^{(i-1)}}{(i-1)!}\right) \quad (26)$$

The steps can be justified similar to (14) - (18). The closed form of the integral in (25) is given in [18, (2.33)].

V. Performance Comparison

To quantify the performance gain of JD in comparison to MSC and MRC in terms of the outage probability, we evaluate the average system transmit SNR P_T/N_0 in (4) to achieve a target outage probability P^{out}_*. Thus we substitute (4) into (12), (18) and (26) for JD, MSC and MRC, respectively, yielding

$$\frac{P_T}{N_0} = \sigma_i(P^{\text{out}}_*), \quad (27)$$

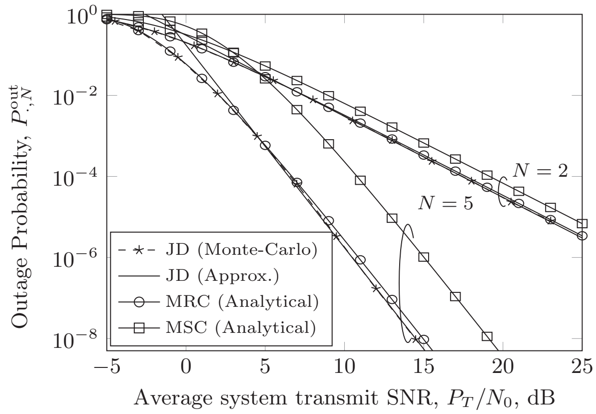

Fig. 3: Outage probability for JD, MRC and MSC with $N \in \{2, 5\}$.

where $\sigma_i(P^{\text{out}}_*)$ is the required average system transmit SNR depending on P^{out}_* and the combining algorithm, $i \in \{\text{JD}, \text{MSC}, \text{MRC}\}$. In order to examine the SNR gain provided by JD versus MRC and MRC, we consider the reduction of the required average system transmit SNR while achieving the same target outage probability. The SNR gain is given by

$$G_{\text{JD},i} = \frac{\sigma_i(P^{\text{out}}_*)}{\sigma_{\text{JD}}(P^{\text{out}}_*)} \text{ for } i \in \{\text{MSC}, \text{MRC}\}. \tag{28}$$

VI. Numerical Results

In this section we illustrate and discuss the outage probability for JD, MSC and MRC. The outage probabilities are assessed in an asymptotic fashion, as well as via Monte-Carlo integration (JD) or an analytical solution (MSC and MRC). For illustration purpose, we assume a binary phase-shift keying modulation and a channel-code rate of $1/2$, such that $R_\text{c} = 0.5$. Moreover, we assume a path loss exponent of $\eta = 3.5$. To ensure a fair comparison, we make use of the total transmit power constraint in (4), i.e., the transmit power is equally allocated to all links, $P_i = {}^{P_T}/_{N}$.

Fig. 3 depicts the exact and approximated outage probability $P^{\text{out}}_{\text{JD},N}$ for JD in (11) and (12), respectively, and the outage probability for MSC $P^{\text{out}}_{\text{MSC},N}$ in (18), and for MRC $P^{\text{out}}_{\text{MRC},N}$ in (26), versus the average system transmit SNR ${}^{P_T}/_{N_0}$. We show results for $N \in \{2, 5\}$. The following can be observed: (i) our JD asymptotic expression in (12) is tight at medium to high SNR; (ii) JD outperforms MSR and MRC, and (iii) the outage probabilities of JD and MRC are tight at low SNR. Based on the last observation, we use the closed-form expression in (26) to adjust the approximation in (12) by an upper bound, i.e.,

$$P^{\text{out}}_{\text{JD},N} \leq \min\left(\frac{A_N}{\bar{\Gamma}^N}, 1 - \exp\left(-\frac{A_1}{\bar{\Gamma}}\right)\left(\sum_{i=1}^{N} \frac{({}^{A_1}/_{\bar{\Gamma}})^{(i-1)}}{(i-1)!}\right)\right), \tag{29}$$

for $\bar{\Gamma}_1 = ... = \bar{\Gamma}_N = \bar{\Gamma}$. We can use the min-operation, since we know that MRC is suboptimal in comparison to JD [19], such that the JD outage probability is less than or equal to the MRC outage probability. In the following the JD outage probability is assessed by (29).

Fig. 4a, Fig. 4b and Fig. 4c depict the required average system transmit SNR ${}^{P_T}/_{N_0} = \sigma_i(P^{\text{out}}_*)$ to achieve the target outage probability for JD, MSC and MRC, respectively, given in (27), versus the number of links. The following can be observed: (i) for JD and MRC to achieve a targeted outage probability the required average system transmit SNR decreases with an increasing number of links; and (ii) for MSC an optimal number of links exists to minimize the required average system transmit SNR for a targeted outage probability. The last observation can be reasoned by the fact that an increasing numbers of links yield a diversity order increase but simultaneously decreases the transmit power per links. A similar study of optimal operating points for MSC can be found in [20].

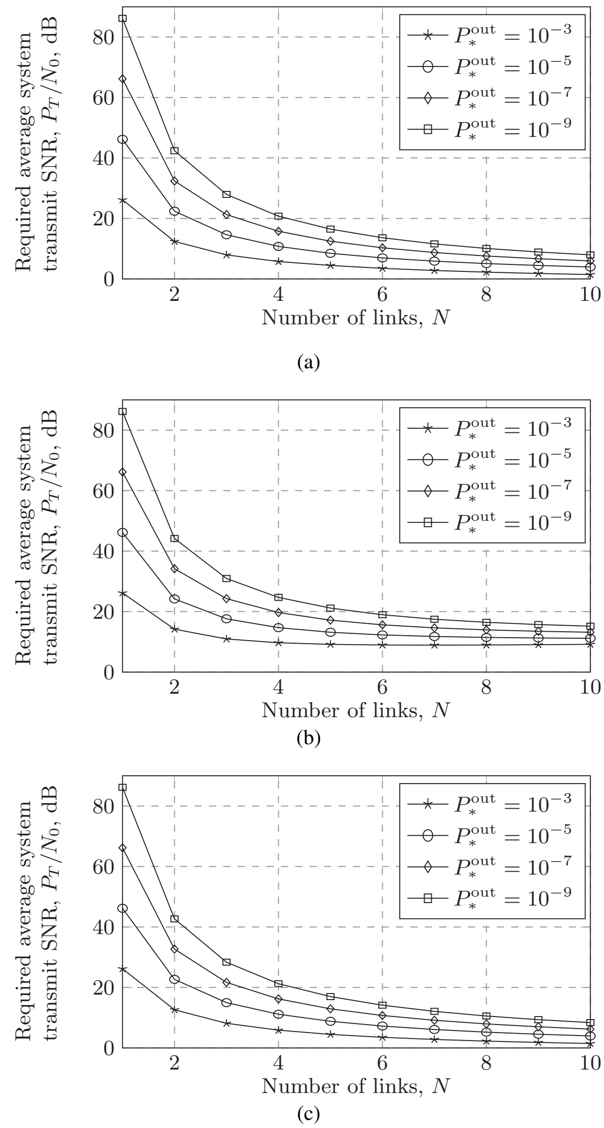

Fig. 4: Required average system transmit SNR for target outage probability for (a) JD, (b) MSC, and (c) MRC.

Fig. 5a and Fig. 5b depict the SNR gain of JD $G_{\text{JD},i}$ in comparison to MSC and MRC, respectively, given in (28), versus the number of links. The following can be observed: (i) JD outperforms MSC and MRC; (ii) for MSC, with every additional link the SNR gain increases; and (iii) for MRC,

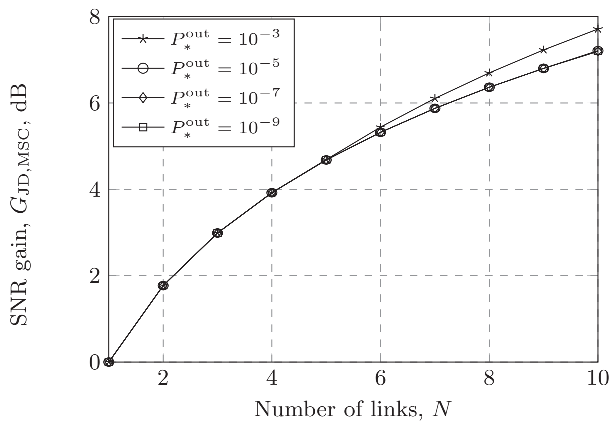

(a)

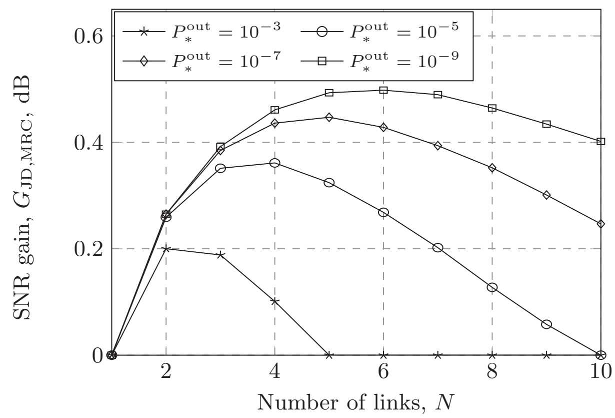

(b)

Fig. 5: Gain of required average system transmit SNR for target outage probability for (a) MSC and (b) MRC.

a maximum exists which depends on the number of links and targeted outage probability. The last observation can be reasoned by considering the outage probability of JD and MRC at low SNR. If the number of links increases, less average system transmit SNR is required, i.e., the system approaches low SNR regime. As observed in Fig. 3 the outage probability of JD and MRC come close at low SNR.

VII. Conclusion

In this work we have derived and evaluated the outage probability for different combining algorithms, namely, joint decoding, maximum selection combining, and maximum ratio combining in the context of multi-connectivity. The outage analysis has been based on the Slepian-Wolf theorem and the source-channel separation theorem. For all three combining algorithms, we have established a remarkably simple, yet accurate analytical framework to describe the outage probability depending on the number of links, the modulation scheme, the code rate, and the received SNR. We have used the analytical framework to compare the performance and thereby have evaluated the reduction of the required SNR when using joint decoding in comparison to maximum selection combining and maximum ratio combining while achieving the same outage probability.

References

[1] P. Schulz, M. Matthe, H. Klessig, M. Simsek, G. Fettweis, J. Ansari, S. A. Ashraf, B. Almeroth, J. Voigt, I. Riedel, A. Puschmann, A. Mitschele-Thiel, M. Muller, T. Elste, and M. Windisch, "Latency critical IoT applications in 5G: Perspective on the design of radio interface and network architecture," *IEEE Communications Magazine*, vol. 55, no. 2, pp. 70–78, Feb. 2017.

[2] D. Öhmann, "High reliability in wireless networks through multi-connectivity," Ph.D. dissertation, TU Dresden, Germany, 2017.

[3] M. Eriksson, "Dynamic single frequency networks," *IEEE Journal on Selected Areas in Communications*, vol. 19, no. 10, pp. 1905–1914, Oct. 2001.

[4] P. Marsch and G. P. Fettweis, *Coordinated Multi-Point in Mobile Communications: from Theory to Practice*. Cambridge University Press, 2011.

[5] A. Ravanshid, P. Rost, D. S. Michalopoulos, V. V. Phan, H. Bakker, D. Aziz, S. Tayade, H. D. Schotten, S. Wong, and O. Holland, "Multi-connectivity functional architectures in 5G," in *Proc. IEEE International Conference on Communications Workshops (ICCW)*, Kuala Lumpur, Malaysia, May 2016, pp. 187–192.

[6] G. Pocovi, B. Soret, M. Lauridsen, K. I. Pedersen, and P. Mogensen, "Signal quality outage analysis for ultra-reliable communications in cellular networks," in *Proc. IEEE Globecom Workshops (GCW)*, San Diego, CA, USA, Dec. 2015, pp. 1–6.

[7] D. Slepian and J. Wolf, "Noiseless coding of correlated information sources," *IEEE Trans. Inf. Theory*, vol. 19, no. 4, pp. 471–480, Jul. 1973.

[8] K. Anwar and T. Matsumoto, "Accumulator-assisted distributed turbo codes for relay systems exploiting source-relay correlation," *IEEE Commun. Lett.*, vol. 16, no. 7, pp. 1114–1117, Jul. 2012.

[9] X. Zhou, M. Cheng, X. He, and T. Matsumoto, "Exact and approximated outage probability analyses for decode-and-forward relaying system allowing intra-link errors," *IEEE Trans. Wireless Commun.*, vol. 13, no. 12, pp. 7062–7071, Dec. 2014.

[10] A. El Gamal and Y.-H. Kim, *Network Information Theory*. Cambridge: Cambridge University Press, 2011.

[11] A. Wolf, D. C. González, M. Dörpinghaus, L. L. Mendes, J. C. S. Santos Filho, and G. Fettweis, "Outage analysis for decode-and-forward multirelay systems allowing intra-link errors," *accepted for publication in IEEE Wireless. Commun. Lett.*

[12] D. C. González, A. Wolf, L. L. Mendes, J. C. S. Santos Filho, and G. Fettweis, "An efficient power allocation scheme for multirelay systems with lossy intra-links," *IEEE Trans. Commun.*, vol. 65, no. 4, pp. 1549–1560, Apr. 2017.

[13] A. Goldsmith, *Wireless Communications*. Cambridge University Press, 2005.

[14] B. Van Laethem, F. Quitin, F. Bellens, C. Oestges, and P. De Doncker, "Correlation for multi-frequency propagation in urban environments," *Progress In Electromagnetics Research Letters*, vol. 29, pp. 151–156, 2012.

[15] T. Cover, "A proof of the data compression theorem of Slepian and Wolf for ergodic sources (corresp.)," *IEEE Trans. Inf. Theory*, vol. 21, no. 2, pp. 226–228, Mar. 1975.

[16] A. Wolf, P. Schulz, D. Öhmann, M. Dörpinghaus, and G. Fettweis, "Diversity-multiplexing tradeoff for multi-connectivity and the gain of joint decoding," 2017. [Online]. Available: http://arxiv.org/abs/1703.09992

[17] D. Brennan, "Linear diversity combining techniques," *Proceedings of the IRE*, vol. 47, no. 6, pp. 1075–1102, 1959.

[18] T. M. Duman and A. Ghrayeb, *Coding for MIMO Communication Systems*. John Wiley & Sons, 2008.

[19] A. F. Molisch, *Wireless Communications*. John Wiley & Sons, 2012.

[20] D. Öhmann, M. Simsek, and G. P. Fettweis, "Achieving high availability in wireless networks by an optimal number of Rayleigh-fading links," in *Proc. IEEE Globecom Workshops (GCW)*, Austin, TX, USA, Dec. 2014, pp. 1402–1407.